Fabrication of sawtooth diffraction gratings using nanoimprint lithography

Chih-Hao Chang,[a] R. K. Heilmann, R. C. Fleming, J. Carter, E. Murphy, and M. L. Schattenburg
Massachusetts Institute of Technology, 77 Mass Avenue, Room 37-420, Cambridge, Massachusetts 02139

T. C. Bailey and J. G. Ekerdt
Texas Materials Institute, University of Texas at Austin, Austin, Texas 78759

R. D. Frankel
Chromaplex, Inc., 15 Lucius Gordon Drive, Suite 115, West Henrietta, New York 14586

R. Voisin
Molecular Imprints, Inc., 1807-C West Braker Lane, Austin, Texas 78758

(Received 25 June 2003; accepted 29 September 2003; published 5 December 2003)

We report a process which integrates interference lithography, nanoimprint lithography, and anisotropic etching to fabricate replicated diffraction gratings with sawtooth profiles. This new process greatly reduces grating fabrication time and cost, while preserving the groove shape and smoothness. Relief gratings with 400 nm period inverted triangular profiles and 200 nm period gratings with 7° blaze angle were replicated from silicon masters with surface roughness of less than 1 nm. This process was developed for fabricating the off-plane blazed diffraction gratings for the NASA Constellation-X x-ray telescope. © *2003 American Vacuum Society.*
[DOI: 10.1116/1.1627814]

I. INTRODUCTION

High efficiency diffraction gratings are important in a variety of applications, such as optical telecommunications, lithography, and laboratory spectroscopy.[1] Special interest has been placed on blazed diffraction gratings for their ability to enhance diffraction intensity at the specular reflection angle. Fabrication of blazed diffraction gratings with spatial periods in the order 0.1–1 μm has thus been an interesting area of research.

Traditional blazed gratings have been mechanically scribed by diamond-tip ruling engines.[2] However, this process is slow and the grating groove suffers from rough surfaces, rounded edges, and numerous other problems. Blazed gratings can also be fabricated using directional interference lithography to obtain a blazed resist profile, followed by ion etching to transfer the pattern into the substrate.[3] Challenges arise when trying to match the etch rates of resist and substrate, and any roughness on the resist surface will transfer to the substrate. Another fabrication process patterns gratings on off-cut (111) wafers with interference lithography, followed by anisotropic etching to achieve blazed grating profiles.[4] This process results in groove surfaces being atomically smooth and blazed at the desired angle. However, since the blazed angle is determined by the off-cut angle, specially oriented wafers must be used. For large grating areas, such as required for NASA's Constellation-X x-ray telescope, the fabrication process can be costly and time consuming. By integrating this process with nanoimprint lithography (NIL), fabrication of blazed diffraction gratings can be tremendously eased.

[a]Electronic mail: chichang@mit.edu

NIL is a promising lithographic technique for replicating patterns on the nanometer scale.[5] We report an application of so-called step-and-flash imprint lithography (SFIL).[6] In this technique a UV-transparent mandrel with an etched pattern is pressed into a low-viscosity UV-curable liquid over a substrate. The liquid is cured when exposed to UV light, and after separation a replica of the pattern on the mandrel is imprinted on the substrate. We have developed an alternative SFIL method that utilizes an opaque mandrel and a transparent substrate. The mandrels used for replication are patterned by interference lithography[7] and anisotropically etched into the silicon substrate.[4] We successfully replicated 400 nm period gratings with inverted triangle patterns and 200 nm period gratings with 7° blaze angles over areas in the range of 40 mm$\times$40 mm.

II. MANDREL FABRICATION

The 400 nm period inverted triangular profile grating was fabricated using (100) silicon wafers, using a process depicted in Fig. 1(a). The wafers were coated according to a bilayer resist scheme that consists of 30 nm of silicon nitride, 130 nm of antireflection coating (ARC), and 380 nm of photoresist. This configuration represents a local minimum in reflectivity at the resist–ARC interface. The coated wafers were patterned with 400 nm period grating lines parallel to the [110] direction using interference lithography. The wafers were then reactive-ion etched (RIE) with O_2 and CHF_3 to transfer the grating pattern into ARC and nitride, respectively. RCA clean was used to remove the remaining resist, ARC, and any polymer that formed during the CHF_3 RIE process. Using the nitride as mask, the Si substrates were anisotropically etched in KOH to produce atomically smooth

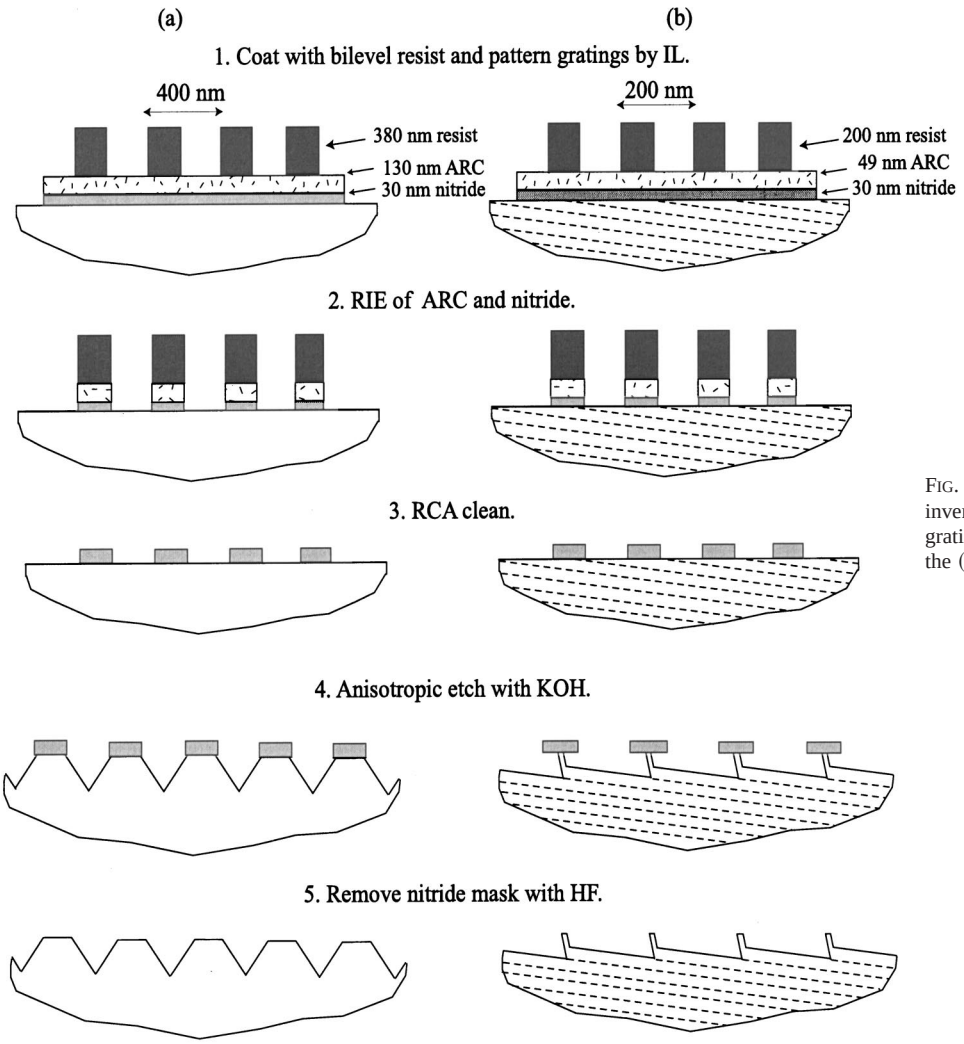

FIG. 1. Fabrication process for (a) 400 nm period inverted triangular grating. (b) 200 nm period grating with 7° blaze angle. The dashed lines are the (111) planes.

facets with angles close to the theoretical value of 54.7°. The nitride mask was then removed in concentrated HF.

A similar process was used to fabricate the 200 nm period blazed gratings, depicted in Fig. 1(b). The wafers used had their surface normal rotated 7° from the [111] direction along the $[1\bar{1}0]$ axis. This angle has a $\pm 0.5°$ tolerance as specified by the vendor. The offcut (111) planes are illustrated in Fig. 1(b). The wafers were coated with 30 nm of silicon nitride, 49 nm of ARC, and 200 nm of photoresist. A thinner resist layer was employed to reduce the aspect ratio of the resist after being developed. The ARC thickness was selected so that the reflected power is at a local minimum at the resist–ARC interface. The wafers were patterned with 200 nm period grating lines parallel to the $[1\bar{1}0]$ direction. The grating pattern was transferred with O_2 and CHF_3 RIE. When these wafers are etched anisotropically in KOH, the offcut (111) planes form the blazed profile. Since the mandrels were anisotropically etched, the surfaces are expected to be atomically smooth. rms roughness of around 0.6 nm were measured using atomic force microscopy (AFM). The finished gratings are shown in Figs. 2 and 3.

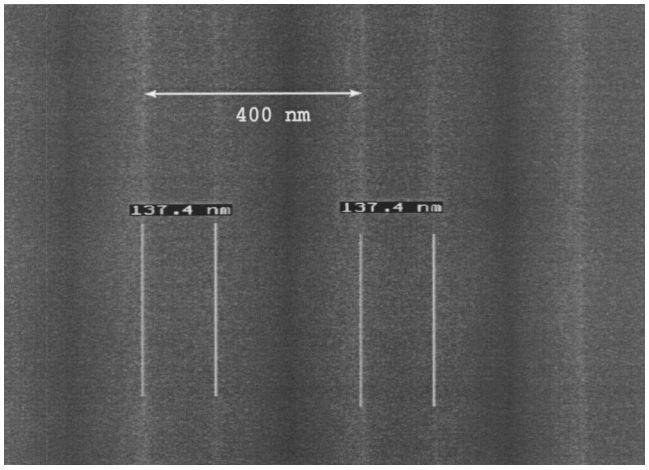

FIG. 2. SEM image of a 400 nm period inverted triangular grating etched anisotropically.

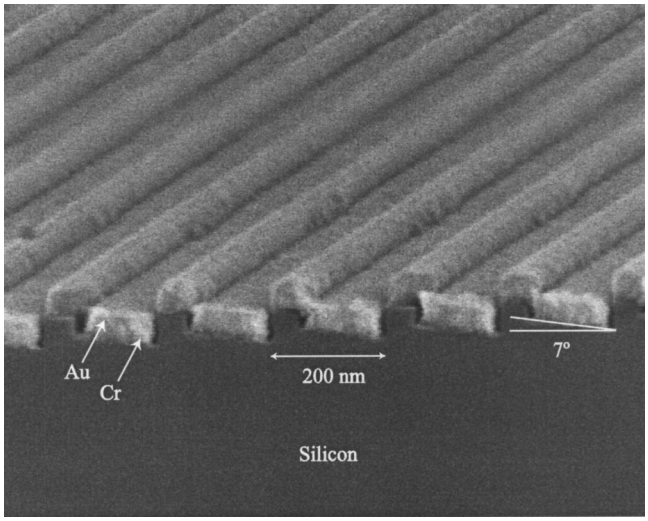

FIG. 3. SEM image of 200 nm period grating with 7° blaze angle, evaporated with 5 nm Cr and 40 nm Au to increase x-ray diffraction efficiency.

III. IMPRINT PROCESS

The silicon gratings were die-sawed into dimensions around 40 mm×40 mm to be used as mandrels for the NIL process. Since silicon exhibits high adhesion energy,[8] a thin film of a low surface energy material such as fluorocarbon is needed to promote release. First, any organic contaminants adsorbed on the surface of the mandrel were cleaned in an UV/ozone chamber for 3 min, and then tridecafluoro-1,2,2,2-tetrahydrooctyltrichlorosilane (FOTS) was vapor evaporated over the mandrel. A thin alkylsilane film forms and is cured at 100 °C for 5 min. After dispensing a drop of polymer precursor, formulated as described by Bailey *et al.*,[9] a fused silica wafer was placed on top of the mandrel. Vacuum suction was utilized to apply the necessary pressure to ensure good contact between mandrel and fused silica wafer. UV light ($\lambda \sim 400$ nm) was then transmitted through the fused silica wafer with a dose of 100 mJ/cm^2 to crosslink the polymer. After separation, the imprinted wafers are coated with Cr and Au to ensure high reflectivity at grazing incidence in the x-ray band.

IV. RESULTS AND DISCUSSION

The replicated gratings show excellent surface uniformity over the area that was imprinted. No apparent release damage was observed over the imprinted area. An image of the replicated 400 nm period inverted triangular grating was scanned using an AFM and is shown in Fig. 4. The surface of the sidewalls has a rms roughness on the order of 0.8 nm. The AFM data was obtained using a multiwall carbon nanotube ($d \sim 20$ nm) mounted on a regular AFM Si tip. The replicated grating exhibits an inverted profile of the mandrel with high conformity. The rounded edges shown on the AFM images may be artifacts due to the tip's finite dimension. SEM images of the same imprinted grating show sharp edges (Fig. 5). The small ripples at the bottom of the imprinted gratings may be caused by the elasticity of the material.

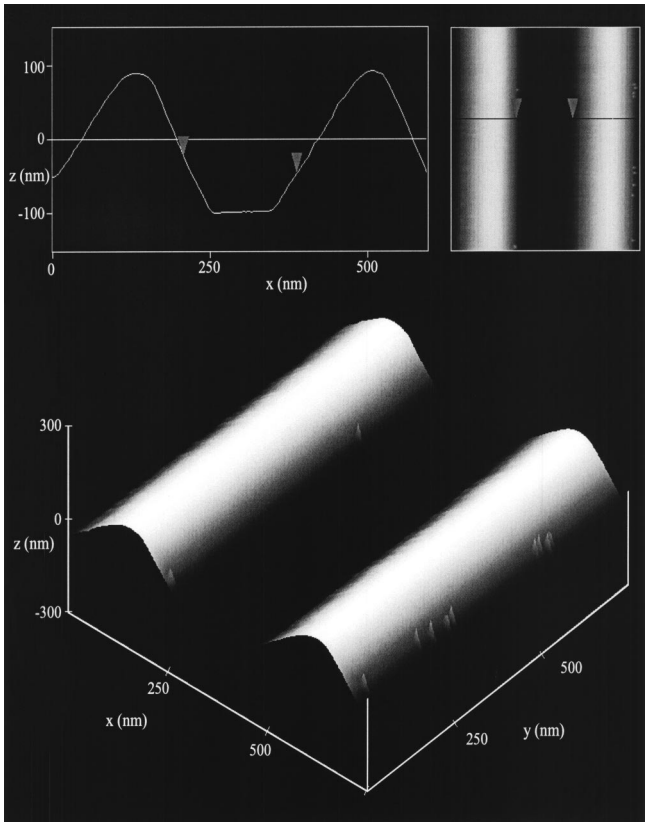

FIG. 4. AFM image of imprinted 400 nm period inverted triangular grating. (a) Cross-section view, (b) 3D view.

Since the ripples are perpendicular to the grating line direction, they could be the result of the polymer stretching and springing back during cleaving of the sample. The micrograph was taken at close proximity to the cleaved edge.

Replication from 200 nm period gratings with 7° blaze angle yielded similar results, as depicted in Fig. 6. Note that there are some ripples in the image caused by noise along the tip scanning direction. The area of greatest interest is the blazed surface, on which the reflection efficiency depends.

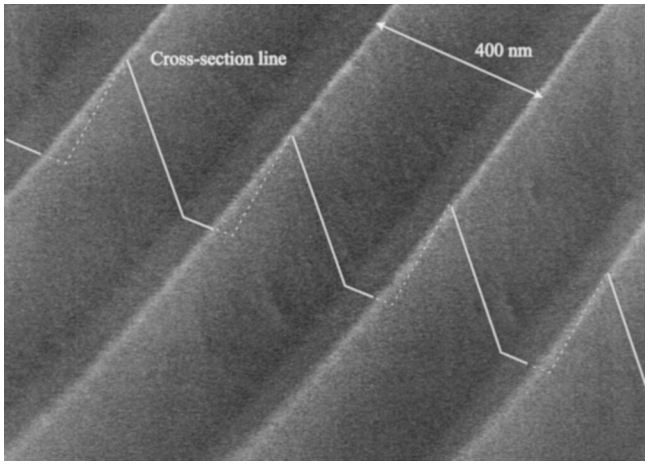

FIG. 5. SEM image of imprinted 400 nm period inverted triangular grating. Sharp edges can be observed. The slight ripples at the base of the triangles may be result of cleaving.

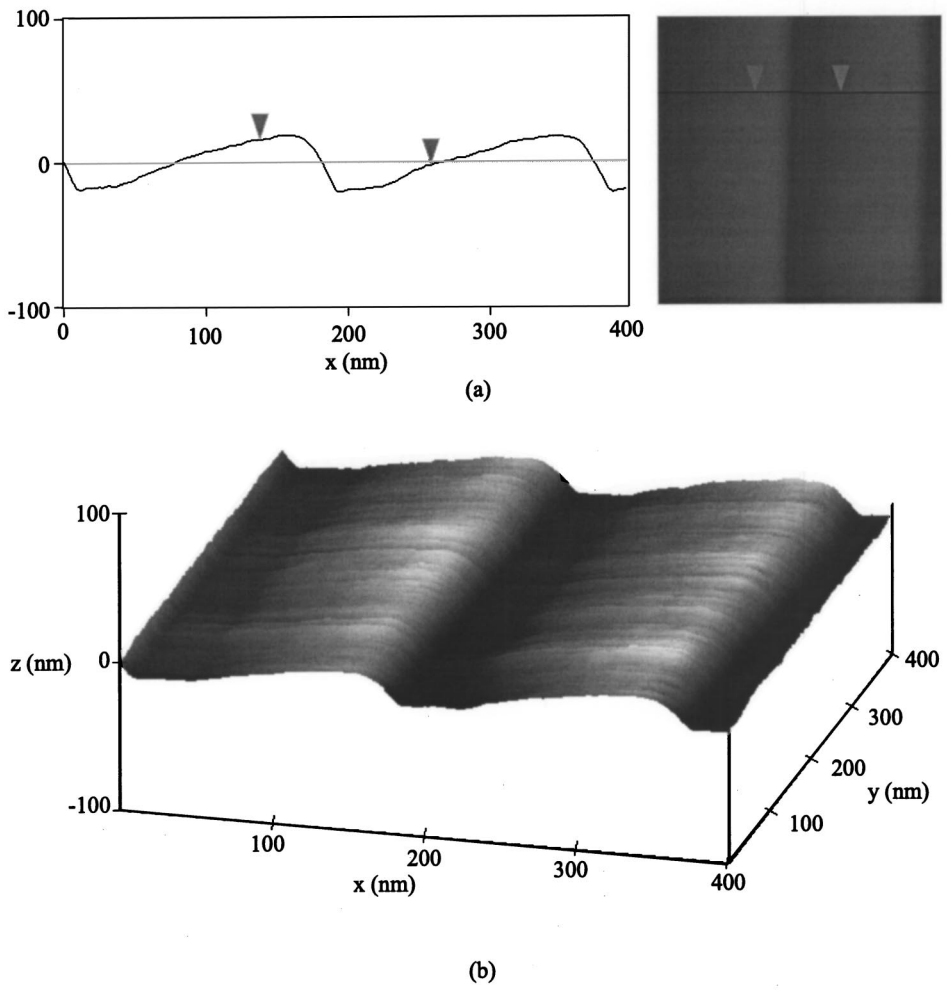

FIG. 6. AFM image of imprinted 200 nm period grating with 7° blaze angle. (a) Cross-section view, (b) 3D view.

The 7° blaze angle is well preserved. The roughness on the blazed surface was measured to have a rms roughness in the order of 0.8 nm. Based on the mandrel, the blazed facet should extend only about 130 nm between grating lines. Examining the AFM image, the slope changes abruptly where the blazed surface stops. The trenches that should be imprinted in the replicas cannot be scanned due to the limitations of the AFM tip. SEM images of another blazed replica sample show high profile imprint fidelity and smooth surfaces (Fig. 7). Some minor edge rounding can be observed.

The inverted profile seen in the replicated grating has a significant advantage over its mandrel for applications in x-ray spectroscopy. For in-plane diffraction gratings where the plane of incidence is normal to grating lines, x rays diffract efficiently only at grazing incidence. The nubs in the mandrel above the blazed surface cause unwanted scattering and strong shadowing.[10] For diffraction gratings in an off-plane mount, where the plane of incidence is parallel to the grating lines, the nub's rectangular wall profile is not blazed and will cause diffracted intensity symmetric about the 0th order, reducing the blazed effect [Fig. 8(a)]. The blazed facets of the imprinted grating leave the optical path of the x rays unblocked, as depicted in Fig. 8(b).

The imprinted gratings demonstrate high imprint pattern conformity, but their efficiency as replacements has yet to be tested. Minor rounding of edges is expected during the imprint process, and can be observed in Fig. 7. The rounding will result in loss of higher order diffraction efficiency. However, the rounding is difficult to quantify, and x-ray diffraction measurements need to be performed. The roughness of the imprinted surface is also not well known. The AFM scans have considerable noise; point and scan defects can be observed in Figs. 4 and 6. The 200 nm period grating with 7° blaze angle, as shown in Fig. 3, was measured to have roughness around 0.6 nm by AFM. The same grating was measured to have high efficiency at an x-ray diffraction testing facility at the University of Colorado.[11] We believe the actual roughness is lower than measured and the AFM roughness results are inconclusive. The replicated gratings seem promising, and x-ray diffraction efficiency measurements are planned for further evaluation.

V. CONCLUSION

We have developed a process which integrates nanoimprint lithography, interference lithography, and anisotropic etching to replicate diffraction gratings with sawtooth patterns. We fabricated 400 nm period gratings with an inverted

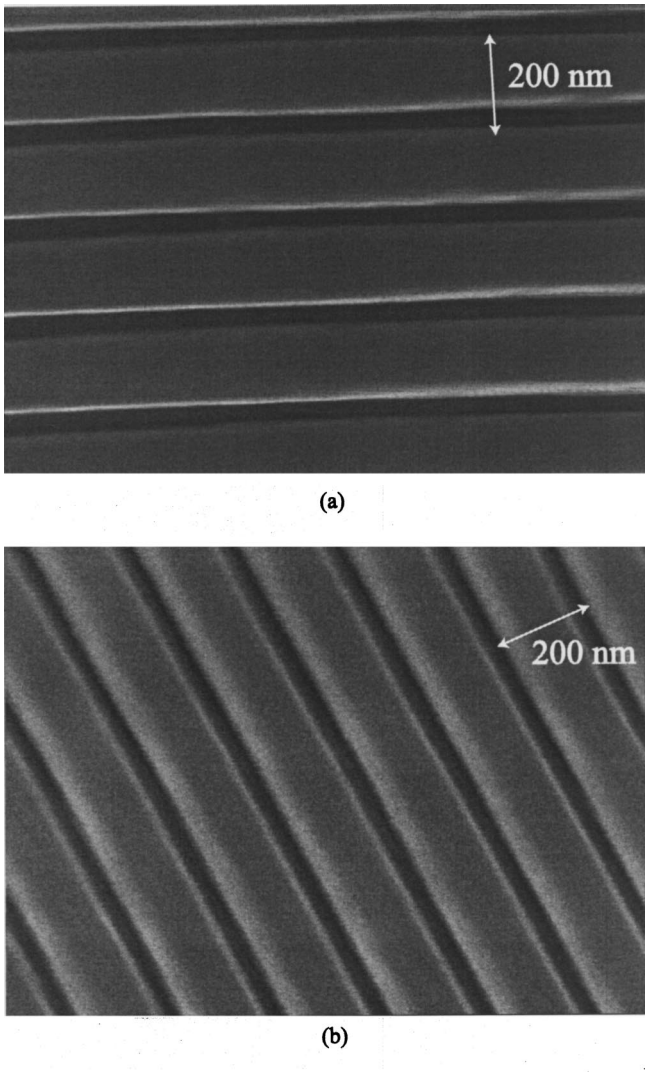

FIG. 7. SEM image of imprinted 200 nm period grating with 7° blaze angle. (a) Top view, (b) tilted view. Smooth surfaces and high imprint fidelity can be seen.

triangular profile and 200 nm period gratings with a 7° blaze angle by imprinting over 40 mm×40 mm area with good uniformity and sub-nm roughness. The process greatly reduces fabrication time and cost. Excellent results have been demonstrated based on the profile conformity of the replica. Diffraction efficiency measurements will be conducted to examine the performance of the replicated gratings.

ACKNOWLEDGMENTS

The authors gratefully acknowledge the outstanding technical assistance of Robert Fleming and Edward Murphy. Student, staff, and facility support from the Space Nanotechnology Laboratory, NanoStructures Laboratory, and Microsystems Technology Laboratory at MIT are also appreciated.

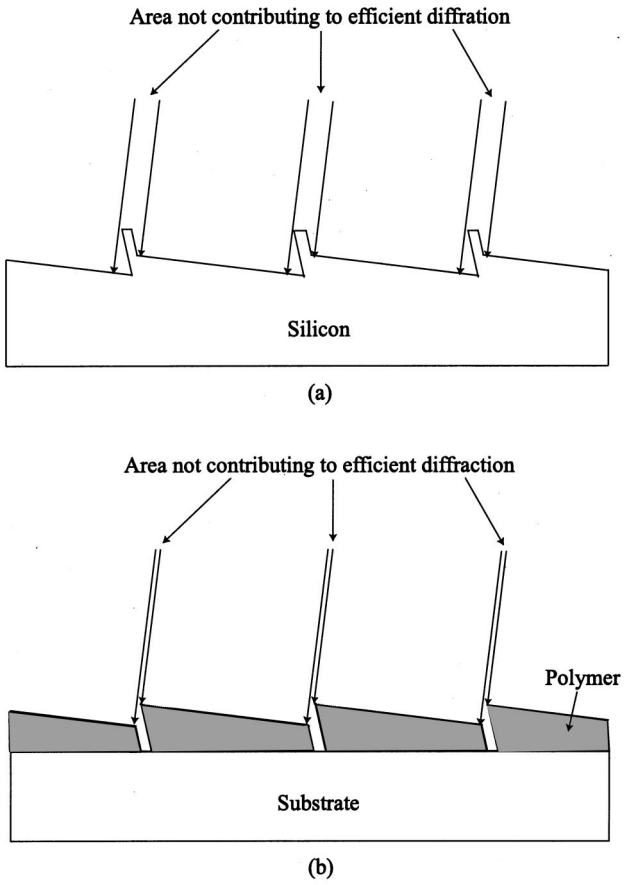

FIG. 8. Drawing of groove geometry showing that the effective diffracting area of the master grating, (a), is less than that of the replicated grating, (b).

This work was supported by NASA Grant Nos. NAG5-12583 and NCC5-633.

[1]E. G. Loewen and E. Popov, *Diffraction Gratings and Applications* (Marcel Dekker, New York, 1997).
[2]J. V. Bixler, C. J. Hailey, C. W. Mauche, P. F. Teague, R. S. Thoe, S. M. Kahn, and F. B. S. Paerels, Proc. SPIE **1549**, 420 (1991).
[3]W. R. Hunter, *Spectrometric Techniques* (Academic, New York, 1985), Vol. IV, p. 63.
[4]A. E. Franke, M. L. Schattenburg, E. M. Gullikson, J. Cottam, S. M. Kahn, and A. Rasmussen, J. Vac. Sci. Technol. B **15**, 2940 (1997).
[5]S. Y. Chou, P. R. Krauss, and P. J. Renstrom, Appl. Phys. Lett. **67**, 3114 (1995).
[6]T. C. Bailey, B. J. Choi, M. Colburn, M. Meissl, S. Shaya, J. G. Ekerdt, S. V. Sreenivasan, and C. G. Willson, J. Vac. Sci. Technol. B **18**, 3572 (2000).
[7]M. L. Schattenburg, E. H. Anderson, and H. I. Smith, Phys. Scr. **41**, 13 (1990).
[8]T. M. Mayer, M. P. de Boer, N. D. Shinn, P. J. Clews, and T. A. Michalske, J. Vac. Sci. Technol. B **18**, 2433 (2000).
[9]T. C. Bailey, S. C. Johnson, S. V. Sreenivasan, J. G. Ekerdt, C. G. Wilson, and D. J. Resnick, J. Photopolym. Sci. Technol. **15**, 481 (2002).
[10]P. Vincent, M. Neviere, and D. Maystre, Appl. Opt. **18**, 604 (1979).
[11]R. L. McEntaffer, S. N. Osterman, A. Shipley, and W. C. Cash, Proc. SPIE EUV, X-ray, and Gamma-Ray Astronomy (submitted).